Reports

Tidal Currents and Eddy Statistics From Iceberg Trajectories off Labrador

Abstract. *Extensive data on the trajectories of icebergs located off the coast of Labrador has yielded information on tidal currents, the effect of wind on iceberg motion, and the properties of the low-frequency eddies. Statistical properties of the data were shown to be related to theoretical ideas on two-dimensional turbulence and to the connection between Eulerian and Lagrangian velocity statistics. The results have led to an estimate of the cross-shelf mixing rate and a statistical prediction scheme for iceberg trajectories.*

Moving icebergs are a hazard to drilling platforms used in the search for oil and gas in some offshore regions of Eastern Canada. It is thus important to predict the future trajectories of icebergs so that those presenting a threat to operations can be towed clear, or preparations can be made for moving the drilling platform (*1*).

During the last decade, the oil industry has collected extensive data on the trajectories of icebergs within about 50 km of numerous well sites off the Labrador coast. We examined many of these data sets and found that they contain information of general oceanographic significance.

The basic observations consist of successive values of radar range and bearing of individual icebergs, at approximately hourly intervals. More than 2000 trajectories obtained from 27 well sites off the coast of Labrador during the summer months of 1973 to 1981 were available to us (*2*). In this report we confine our attention to two of the larger data sets, one from site GUDRID H-55 at 54°54′30″N, 55°52′32″W in 299 m of water and the other from site RUT H-11 at 59°10′16″N, 62°16′47″W in 126 m of water (Fig. 1). The data were edited by examining individual tracks and eliminating those of icebergs that grounded or were towed and by correcting or deleting extreme outliers in a histogram of speeds. The edited data consist of 6145 values of velocity (from changes in position), position, and time, denoted (***u***, ***x***, *t*), from 197 separate trajectories for GUDRID, spanning 85 days from 10 July 1974. Figure 2 shows examples of trajectories that illustrate the spatial variability. For RUT, our edited data consist of 3644 values of (***u***, ***x***, *t*) from 124 trajectories spanning 70 days from 14 July 1981.

Tidal currents can contribute significantly to iceberg motion. We performed a least-squares fit to the data of the three main semidiurnal constituents, M_2, S_2, and N_2, and the two main diurnal constituents, K_1 and O_1 (*3*). Weaker constituents are below the noise level, and this contributes an uncertainty of about ±15 mm/sec in the analyzed constituents (from a study of the level of the residual energy spectrum near the tidal frequencies). Table 1 shows the results for the main semidiurnal tide, M_2, at RUT and a comparison with results from current meter data obtained at a nearby location during 76 days in 1980 (*4*) and from a 2-day record at the drillship itself (*5*). The agreement in ellipse inclination and Greenwich phase lag is remarkable. The current meter data show a decrease in speed with depth, but not much change in inclination and phase, and show that the icebergs respond to the average tidal currents in the top few tens of meters of the ocean (*6*). The iceberg-derived speeds in the four quadrants and at the mooring location appear to be inversely correlated with water depth, although the variation is small. Within the limita-

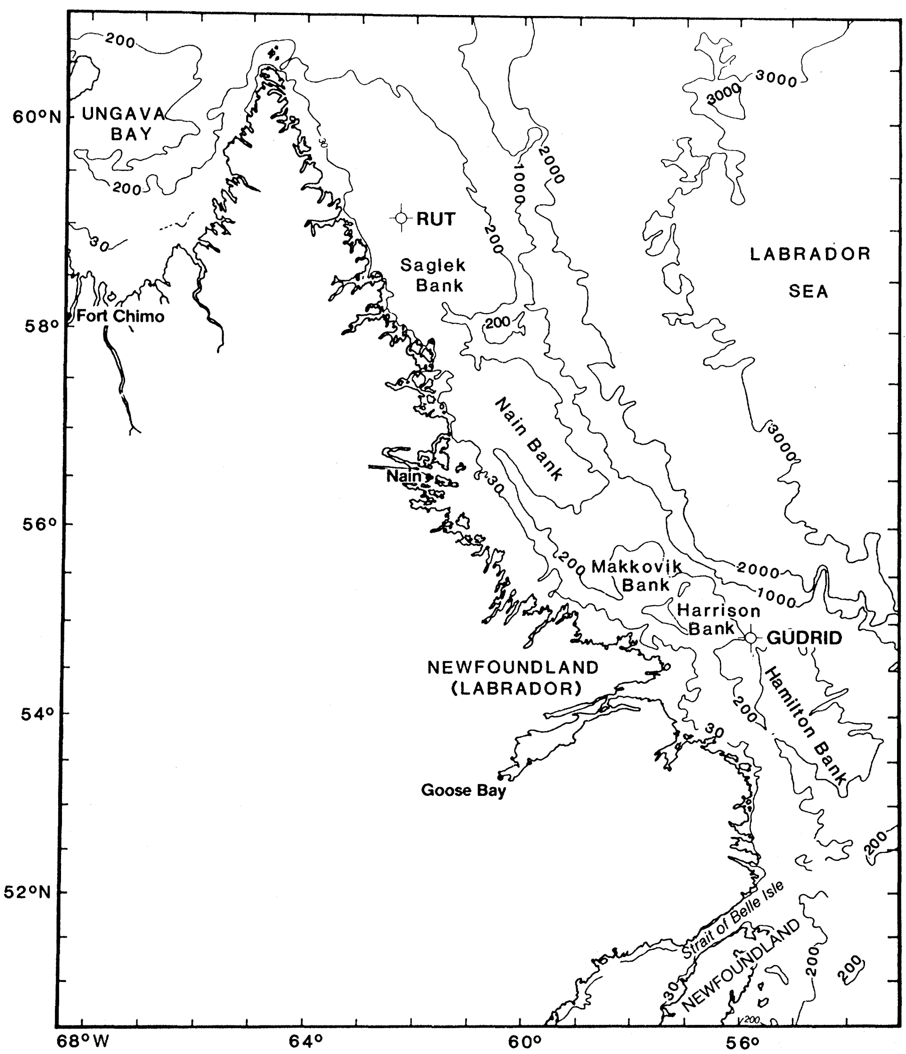

Fig. 1. The continental shelf off Labrador, showing the location of well sites GUDRID and RUT. Isobath depths are in meters.

tions imposed by the noise level, the agreement between iceberg and current meter estimates is also good for other tidal constituents.

Similar comparisons were carried out for GUDRID and other locations, although the tides are much smaller than at the RUT site on Saglek Bank.

For the GUDRID site, we obtained values of geostrophic wind at 6-hour intervals (*7*); we reduced these wind values by a factor of 0.7 and rotated them counterclockwise by 15° to obtain surface winds (*8*). Interpolated values were then used in a cross-correlation with the iceberg velocities. The correlations are a maximum at zero time lag, with values of 0.30 between u_W and u_I, 0.39 between v_W and v_I, -0.01 between u_W and v_I, and -0.08 between v_W and u_I, where W is wind, I is iceberg, u is in the eastward direction, and v is in the northward direction. After allowing for temporal autocorrelation in the wind data and also for the noise and time and space correlations in the iceberg data (see later), we estimate that any wind-iceberg velocity correlation above 0.14 is significant at the 95 percent level. The cross-correlations between orthogonal wind and iceberg velocity components are then insignificant; the correlations between components in the same direction are consistent with a downwind iceberg drift of about 1.8 ± 0.7 percent of the wind speed. This downwind motion and percentage are consistent with other estimates from a few individual tracks and a balance of quadratic drag laws (*9*). The substantial draft of the icebergs appears to prevent a response to the water very near the surface, which may have a larger response to wind and an Ekman drift to the right of the wind.

Before computing other properties of the data, we removed the mean flow, defined as the average for all the data when wind effects (1.8 percent of the wind speed) and tidal currents are removed. At the GUDRID site this mean flow has eastward and northward components (21,−42) mm/sec; the wind-driven component adds a further (34,6) mm/sec to give a mean iceberg drift of (55,−36) mm/sec. The mean flow and variance are not significantly different for the four quadrants around the well site; the residuals (u', v'), with overall mean flow, wind effects and tide removed, have $\overline{u'^2}$ and $\overline{v'^2}$ approximately equal at 0.030 and 0.032 m^2/sec^2. Moreover, $\overline{u'v'} = -7 \times 10^{-4}$ m^2/sec^2, not significantly different from zero. We conclude that the flow in the vicinity of GUDRID is reasonably homogeneous and isotropic.

The residual velocity field has an autocorrelation function shown in Fig. 3. It has been scaled up by 50 percent so that the autocorrelations $R_{u'u'}(\tau)$ and $R_{v'v'}(\tau)$ are equal to 1 at small lag τ. This is equivalent to assigning 0.01 m^2/sec^2 of the variance to noise; at a typical 1-hour interval between observations, this is equivalent to a root-mean-square position error of 360 m. There is evidence for

Table 1. Comparison of the M_2 tidal ellipse computed from iceberg trajectories in the four quadrants about the well site, for all the data, and for trajectories within 10 km of the mooring location (MI) 32 km south-southeast of the well site at 58°53.3′N, 62°10.3′W. The other data are for two current meters (MC) at the mooring location and two (RUT) at the drillship. The inclination is the angle counterclockwise from due east of a semimajor axis, and the Greenwich phase lag gives the time at which the current vector is along the axis. All data sets show a clockwise rotation of the current vector.

Data	Instrument depth (m)	Water depth (m)	Semi-major speed (mm/sec)	Semi-minor speed (mm/sec)	Inclination (deg)	Greenwich phase lag (deg)
NE	Icebergs	144	247	97	149	331
NW	Icebergs	131	286	110	137	334
SW	Icebergs	146	238	79	131	332
SE	Icebergs	149	222	89	140	333
All	Icebergs	149	249	95	140	333
MI	Icebergs	168	181	76	143	338
MC	62	179	134	41	140	345
MC	170	179	115	38	110	319
RUT	20	126	270	120	121	340
RUT	40	126	149	20	120	345

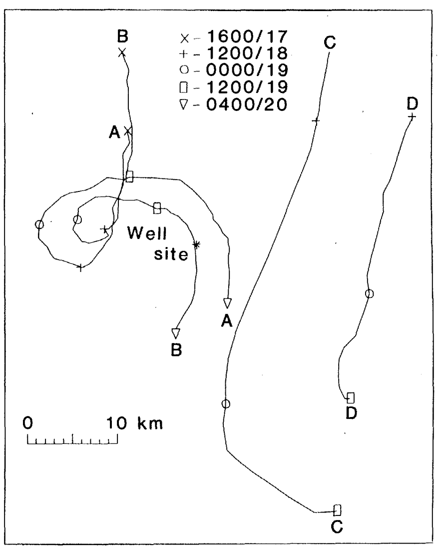

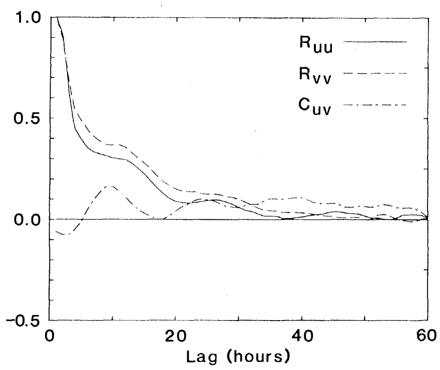

Fig. 2 (left). Four iceberg trajectories observed from GUDRID. Symbols show positions at hour and date in July 1974. Fig. 3 (right). Autocorrelation of the residual velocity field for GUDRID, obtained by averaging all contributions to bins with ranges (0,1), (1,3), (3,5), ··· hours, and scaling to give $R_{u'u'} = R_{v'v'} = 1$ as $\tau \rightarrow 0$. The cross-correlation is defined as $C_{u'v'}(\tau) = \frac{1}{2}[u'(t)v'(t + \tau) - u'(t + \tau)v'(t)]$.

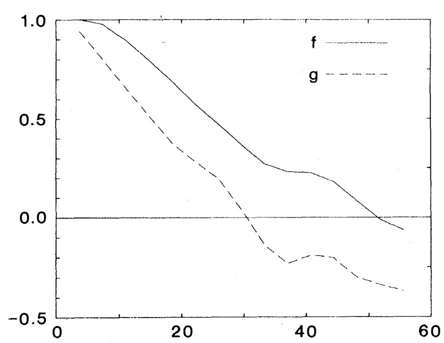

Fig. 4. Spatial dependence in a separated form of the Eulerian velocity cross-correlations: $f(r)$, longitudinal; $g(r)$, transverse.

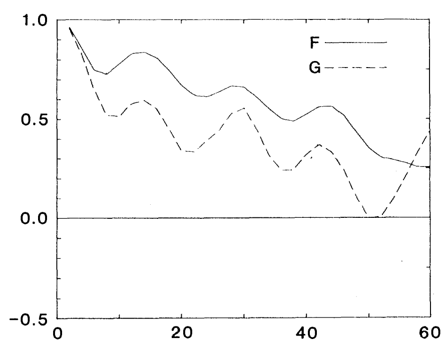

Fig. 5. Time dependence in a separated form of the Eulerian velocity cross-correlations: $F(\tau)$, longitudinal; $G(\tau)$, transverse.

weak inertial oscillations (the local inertial period is 14.8 hours), but otherwise $R_{u'u'}$ and $R_{v'v'}$ fall off more or less exponentially with time, with an *e*-folding time of 15 hours. The lagged cross-correlation between u' and v' shows the weak clockwise-rotating inertial oscillations and an indication of more counterclockwise than clockwise energy at lower frequencies.

The autocorrelations lead to a particularly simple statistical scheme for operational trajectory prediction (*10*) and also imply a horizontal diffusivity (*11*) of 1100 m^2/sec on this part of the Labrador Shelf. This estimate is slightly in error because the influence of the wind prevents the icebergs from following the current perfectly. Using length scales determined from an Eulerian analysis (see below), we estimate that this has reduced the Lagrangian autocorrelation time by about 1 hour, so that the eddy diffusivity should be about 1200 m^2/sec.

We have more than 6000 values of the residual velocity (u', x, t) at GUDRID. We first referred these to a frame of reference moving with the mean flow and then evaluated the correlation functions $f\star(r,\tau)$, $g\star(r,\tau)$ of longitudinal and transverse velocity components, respectively (*12*), for spatial separation r and time lag τ. In doing this we multiplied together all velocity pairs for different icebergs and accumulated them in bins of size 2 hours (as for the autocorrelation) by 3.7 km. We also evaluated the lagged cross-correlation between longitudinal and transverse velocity components; this shows the effects of inertial motion, but is relatively small and is not discussed further here.

We found that $f\star$ and $g\star$ are reasonably separable into

$$f\star(r,\tau) = f(r)F(\tau)$$

$$g\star(r,\tau) = g(r)G(\tau)$$

These functions are shown in Figs. 4 and 5.

Nondivergent two-dimensional turbulence would have $g = d(rf)/dr$ (*13*), and the data are not inconsistent with this. The length scale of the eddies, from the value of r for which $g(r) = 0$, is 31 km, comparable with the length scale of shelf-edge eddies observed in satellite imagery (*14*).

The integral time scale (from an average of $F(\tau)$ and $G(\tau)$ in Fig. 5) is about 40 hours, considerably longer than the corrected Lagrangian time scale of 16 hours, as predicted theoretically (*15*).

The functions $f\star(r,\tau)$ and $g\star(r,\tau)$, with or without the assumption of separability, can be Fourier-transformed into the wavenumber-frequency energy spectrum of the eddy field (*16*). We emphasize that, as elsewhere (*13*), drifter data can provide information that is not readily obtainable from moored current meters.

CHRISTOPHER GARRETT
JOHN MIDDLETON
MARK HAZEN
FOUAD MAJAESS
Department of Oceanography, Dalhousie University, Halifax, Novia Scotia, Canada B3H 4J1

References and Notes

1. For a general review of the operational problems, see J. D. Miller and M. J. Dillon [*J. Can. Pet. Technol.* **23**, 45 (1984)].
2. Data for 1974 to 1979 were compiled by the Atmospheric Environment Service and were provided to us by S. D. Smith of Bedford Institute. J. R. Buckley of PetroCanada provided the data for 1980 and 1981.
3. Correction for nodal factors and conversion to Greenwich phase lag follow the procedure described in the tidal manual of the Canadian Hydrographic Service.
4. D. B. Fissel and D. D. Lemon, "Analysis of physical oceanographic data from the Labrador shelf, summer 1980" (report published by Arctic Sciences Ltd., Sidney, British Columbia, 1982), vols. 1 and 2.
5. J. R. Buckley, personal communication.
6. Draft estimates were made for about 25 percent of the icebergs tracked, giving a mean draft of 75 m; this is probably an overestimate (J. D. Miller, personal communication).
7. V. R. Swail and A. Saulesleja, "Geostrophic wind climatology of the Northwest Atlantic Ocean" (Canadian Climate Centre Report 81/6, 1981). A data tape was provided to us by B. D. Petrie of Bedford Institute.
8. K. R. Thompson, R. F. Marsden, D. G. Wright, *J. Phys. Oceanogr.* **13**, 1003 (1983).
9. S. D. Smith and E. G. Banke, *Cold Regions Sci. Technol.* **6**, 241 (1983).
10. C. J. R. Garrett, *Iceberg Res.* **7**, 3 (1984).
11. G. I. Taylor, *Proc. London Math. Soc. Ser. A*, **20**, 196 (1921).
12. G. K. Batchelor, *The Theory of Homogeneous Turbulence* (Cambridge Univ. Press, Cambridge, 1960).
13. H. J. Freeland, P. B. Rhines, T. Rossby, *J. Mar. Res.* **33**, 383 (1975).
14. P. H. LeBlond, *Atmos.-Ocean* **20**, 129 (1982).
15. J. F. Middleton, *J. Mar. Res.* in press.
16. ——— and C. J. R. Garrett, in preparation.
17. We thank numerous anonymous ice observers who collected the original data provided to us by S. D. Smith and J. R. Buckley. We thank S. D. Smith, J. R. Buckley, J. D. Miller, and B. D. Petrie for discussions. Supported by a contract from the Department of Supply and Services and by the Natural Sciences and Engineering Research Council.

25 July 1984; accepted 22 October 1984

Rheology of Glacier Ice

Abstract. *A new method for calculating the stress field in bounded ice shelves is used to compare strain rate and deviatoric stress on the Ross Ice Shelf, Antarctica. The analysis shows that strain rate (per second) increases as the third power of deviatoric stress (in newtons per square meter), with a constant of proportionality equal to 2.3 × 10^{-25}.*

Glaciers flow under gravitationally induced stresses. The weight of the ice causes the glacier to spread and thin in a manner dictated by surface conditions, basal conditions, and the ice constitutive relation between strain rate and applied stress. Because of the complex interaction of these three elements within the glacier and because of the difficulty of simulating intraglacial conditions in the laboratory, the constitutive relation is still an issue in glaciology.

Laboratory investigations (*1, 2*) have yielded a power-law relation between the steady-state effective strain-rate ($\dot{\epsilon}$) and the effective deviatoric stress (τ), such that

$$\dot{\epsilon} = A\tau^n \qquad (1)$$

where $\dot{\epsilon}$ and τ are defined so as to be invariant under coordinate system rotation (*3*). The ice-flow law constant A is affected by ice fabric and impurity content and exhibits an Arrhenius-type temperature dependence. The value of n is approximately 3, but laboratory experiments are inconclusive for $\tau < 1$ bar and at temperatures less than -10°C—the typical stress and temperature regime of polar glaciers—because strain rates are very small and it is difficult to distinguish steady-state creep from transient creep. Consequently, information on the low-stress rheology of ice is best obtained from observations of glacier behavior. These observations are needed also to detect whether the fabric of glacier ice (grain size, crystal orientation, and so on) significantly affects ice rheology.

Studies of the closure of boreholes and tunnels in glacer ice (*3*) and of ice-rise morphology (*4*) have yielded in situ estimates of A and n. Results are ambiguous, however, due mainly to uncertainties in associated estimates of basal temperatures and of stresses within the ice. Less ambiguous results have been obtained from ice shelves—floating platforms of thick ice that are extensions of the inland ice sheet over the ocean. There is no friction at the base of an ice shelf. Thus, strain rates measured at the surface are characteristic of the entire thickness, and the spreading stress (T) in a freely floating ice shelf can be expressed simply (*5*) in terms of ice thickness (H), the acceleration due to gravity (g) and the densities of seawater (ρ_w) and ice (ρ_i)

$$T = \frac{1}{2}\frac{\rho_i}{\rho_w}(\rho_w - \rho_i)gH \qquad (2)$$